

Cooling of Neutron Stars through Emission of Neutrinos and Photons: Effects of Modified Gravity and Magnetic Field using TOV Equations

Charul Rathod* and M. Mishra

Department of Physics, Birla Institute of Technology and Science, Pilani, Pilani campus-333031, India

Prasanta Kumar Das

Department of Physics, Birla Institute of Technology and Science,

K. K. Birla Goa Campus, NH-17B, Zuarinagar, Sancoale, Goa - 403726, India

(Dated: December 9, 2024)

The existence of dark matter has long been extensively studied in the past few decades. In this study, we investigate the emission of neutrinos and photons from neutron stars (NSs) by employing the modified theory of gravity and the corresponding Tolman-Oppenheimer-Volkoff (TOV) system of equations. The extreme matter density and magnetic field inside the NSs provide a unique laboratory for studying fundamental physics, including the interplay between gravity and quantum field effects. The impact of a strong magnetic field has also been incorporated into the corresponding TOV equations. We here attempt to see how neutrinos and photons emissions from these compact objects are impacted by the modified TOV equations due to modified theory of gravity; $f(R, T)$ gravity or scalar-tensor theory and strong magnetic fields. Our analysis focuses on how these modifications influence the structure, cooling, and photon/neutrino luminosities of NS. We computed the surface temperature of NSs for normal Einstein gravity and modified gravity theories with and without magnetic field for three EoSs; namely APR, FPS and SLY. On comparison of our predicted values of surface temperature with the observed surface temperature for three NSs, we find that modified gravity along with inside magnetic field-based predictions shows reasonable agreement with the corresponding observed values.

PACS numbers:

I. INTRODUCTION

Among the densest and most extreme objects in the universe are neutron stars (NSs) [1]. They are created when, near the end of a giant star's life cycle, the core collapses due to gravity after a supernova explosion. What remains is a highly compact remnant, compacted into a sphere with a radius of only 10 to 20 km and with masses usually between 1.4 and 2 times that of the Sun. Extreme compression of matter thus occurred produces incredibly high densities, frequently more significant than the density of an atomic nucleus. Since neutron stars have an average density of 10^{14} to 10^{15} gm/cm³ [2], one teaspoon of neutron star material would weigh billions of tonnes on Earth. These stars have some of the most vital surface magnetic fields [3] in the universe, with magnitudes as high as $10^{13} - 10^{14}$ Gauss, potent gravitational forces and a tremendous amount of pressure inside.

Neutron stars offer a unique physical environment that makes them an excellent laboratory for examining basic issues regarding the behavior of matter in harsh environments [4]. Atomic nuclei are squashed together in such an environment, and protons [5] and neutrons interact so strongly that it becomes difficult to distinguish between them. Therefore, neutron stars provide a good platform for testing theories related to basic nuclear physics

and gravitational physics [6] especially in environments that are extremely difficult to reproduce in a terrestrial laboratory.

Historically, Einstein's General Relativity theory [7] has been used to explain the composition and behavior of neutron stars. Black holes and the curvature of spacetime around a big astrophysical object are just two examples of the many situations in which the gravitational behavior of astronomical entities has been successfully described by General Relativity, which was developed by Einstein in 1915. The Tolman-Oppenheimer-Volkoff (TOV) equations, which describe the balance of internal pressure and gravitational forces to maintain the equilibrium of a star comprised of degenerate nuclear matter, are the reduction of Einstein's field equations in the setting of neutron stars. Researchers can determine mass-radius connections using these equations, which are essential for comprehending the internal structure of a neutron star. Though general relativity has succeeded in explaining many of the observed results, new astronomical measurements have shown severe problems that could point to the theory's shortcomings, especially when describing cosmic events. The unusual rotational dynamics of Stars and Galaxies, the observable matter distribution in galaxy clusters, and gravitational lensing effects, that cannot be adequately described by relying solely on visible baryonic matter, are a few notable examples of its shortcomings. According to the above mentioned observations, the universe may include enormous amounts of dark matter, an elusive, non-luminous form of matter, or gravity may op-

*Electronic address: charulrathod1813@gmail.com

erate differently on extremely large scales, especially in areas with strong gravitational fields.

Two major approaches have been proposed to account for these discrepancies:

Dark Matter Theories: According to these theories, a type of matter that does not emit or absorb electromagnetic radiation, penetrates the cosmos and is, therefore, unseen so far, even after devoting non-trivial efforts by scientists. Although dark matter does not directly and measurably interact with baryonic matter, it does interact gravitationally, influencing the dynamics of galaxies and clusters. The flattening of galaxy rotation curves, which suggests that galaxies contain more mass than is apparent in their stars and gas, is one phenomenon that the dark matter hypothesis explains. The gravitational lensing effects found in distant galaxies, which imply the influence of invisible massive structures bending light in ways compatible with Einstein’s predictions, can also be explained by the presence of dark matter.

On the other hand, *modified gravity theories* imply that Einstein’s general theory of relativity lacks some essential components. According to these ideas, the conventional explanation of gravity fails in some situations, such as extremely gravitational solid fields, very high densities, or substantial spatial scales, necessitating new physics. The $f(R)$ gravity and Modified Newtonian Dynamics (MOND) [8–11] are two examples that modify the equations of motion to take observable deviations into account without introducing dark matter. These hypotheses are compelling in situations about galaxy dynamics and the early development of the cosmos.

In the current work, we plan to concentrate on modified gravity; as it relates to neutron star associated observations. We plan to study more about the interaction between gravitational physics and the interior characteristics of these compact objects by predicting the behavior of neutron stars in the context of modified gravity[12]. More precisely, we examine how changes to the TOV equations brought about by including new gravitational components or coupling functions can change the predicted characteristics of neutron stars, such as their emission characteristics, mass/pressure profiles and surface temperature.

Neutron Stars and Modified Gravity: The TOV equations characterize hydrostatic equilibrium for spherically symmetric matter distributions and are generalized when studying neutron stars under modified gravity theories [13]. The balance between gravitational forces and the degeneracy pressure of nuclear matter in the conventional TOV formalism determines the star’s maximal mass and internal structure. These equations must be modified if gravity differs from what General Relativity predicts in the presence of the intense pressures and densities seen inside a neutron star. The $f(R)$ gravity [9] is an example of a modified gravity theory in which the Einstein-Hilbert action (the foundation of general relativity) [2, 4–6, 14] is altered by adding a function of the Ricci’s scalar R , which results in extra terms in the field

equations. These parameters can influence the mass distribution inside the star and offer various predictions of how neutron stars maintain stability. Understanding the magnetic field of neutron stars [1] is crucial for comprehending their physical characteristics. Magnetars are a subclass of neutron stars with powerful magnetic fields [15] ranging from 10^{18} Gauss in ordinary pulsars to 10^{15} Gauss in magnetars. The reason is that the magnetic field intensity affects the stiffness of nuclear matter and, in turn, the pressure profile inside the star. It therefore substantially impacts the equation of state (EoS) of matter within the star. These magnetic fields can have an even more noticeable influence when modified gravity is present, resulting in a complex interaction between degeneracy pressure, magnetic pressure, and gravitational forces.

The paper is organized as follows: In Section I, we present a brief introduction. Section II describes the modified TOV equations NSs cooling mechanisms. We have also subsequently discussed neutrino emission rates in this section. In Section III, we present the discussion on the results of the impact of magnetic fields and modified gravity on various observables and macroscopic NS properties. We have discussed how including a magnetic field and modified gravity affects the profiles and cooling rates. Further, we also investigate the luminosities (neutrinos and photons). Finally, in Section IV, we summarize and conclude the work by describing key findings and their possible future implications.

II. FORMALISM

A. Equation of States(EoSs)

Although some part of the formalism used in the current work is common with work done by other researchers [15–17], yet we briefly describe it below to make it self-contained as far as possible. We here begin with enumerating three distinct equations of state (EoSs), namely; APR, FPS, and SLY, which we employed here to solve TOV equations.

APR (Akmal-Pandharipande-Ravenhall) EoS: The APR EoS [18, 19] uses isospin asymmetry [20, 21] and baryon density to model the interaction potential. The transition from the high-density phase (HDP) to the low-density phase (LDP) is captured. An important aspect of comprehending the evolution of neutron stars is this phase change, which notably causes the star to shrink more quickly.

FPS EoS: The inner crust and liquid core of the neutron star are cohesively described by the FPS EoS [22]. The transition between the crust and liquid core is located at $\rho_{\text{edge}} = 1.6 \times 10^{14} \text{ gm/cm}^3$. Prior to this transition, there are a number of weakly first-order phase transitions between various nuclear configurations, each with relative density jumps of less than 1%. When

considering an alternate effective nuclear Hamiltonian, a crucial factor in neutron star matter modeling, the FPS EoS is especially appropriate.

SLY EoS: According to the SLY effective nuclear interaction model, which forms the basis of the SLY EoS [23], the nuclei in the neutron star matter continue to remain spherical in shape all the way to the bottom of the inner crust. When the density reaches $\rho = 1.3 \times 10^{14}$ gm/cm³, a uniform npe (neutron-proton-electron) plasma is formed. The cooling behavior of the star is consistently described by this EoS, particularly in the vicinity of the minimum mass, where the liquid core and solid crust converge. The phase transition between the crust and core is weakly first-order, with a relative density jump of about 1%. The SLY model differs from the FPS EoS by the fact that SLY describes the liquid core (uniform nuclear matter) and the inner crust (nuclear structures) using the same nuclear Hamiltonian. Compared to the FPS EoS, the SLY EoS is stiffer in the area of the crust-core interface. In addition, the SLY scenario exhibits a more noticeable discontinuous stiffening at the crust-core transition than the FPS model.

The interior structure and behavior of neutron stars, especially in relation to the phase transitions between the crust and core, as well as the thermodynamic characteristics of matter at very high densities, are all described differently by these three EoSs.

B. Tolman–Oppenheimer–Volkoff Equations for non-rotating NSs

The internal structure of a spherically symmetric, non-rotating, self-gravitating astrophysical object in hydrostatic equilibrium is described by the Tolman–Oppenheimer–Volkoff (TOV) equations; a system of the first order differential equations [24] that were obtained explicitly from solving Einstein’s field equations in General Relativity. The equilibrium is maintained when the outward pressure forces caused by the degeneracy pressure of the particles within an object precisely balance the inward gravitational force acting on that layer of material. When simulating the characteristics of white dwarfs, neutron stars, and other compact objects, where relativistic effects are crucial to incorporate, the TOV system of equations are of paramount importance [25]. In Schwarzschild’s coordinates, the space-time metric [26] within a spherically symmetric star, non-rotating astrophysical objects, can be expressed as:

$$ds^2 = -\exp(2\phi) c^2 dt^2 + \frac{dr^2}{1 - \frac{2Gm(r)}{rc^2}} + r^2 d\Omega^2, \quad (1)$$

where, ds^2 represents the infinitesimal interval space-time and ϕ is the gravitational potential function, which varies with r . The symbol c denotes the speed of light, t

is the time coordinate, and r is the radial coordinate from the center of the star. The term $m(r)$ denotes the enclosed mass within radius r , and G is the universal gravitational constant. The quantity $d\Omega$ represents the solid angle element in spherical coordinates, given by $d\Omega^2 = d\theta^2 + \sin^2\theta d\varphi^2$, where θ and φ are the angular coordinates.

The functions $\phi(r)$ and the enclosed mass $m(r)$ characterize the gravitational field inside the star. At the star’s surface, where the radius is R and the enclosed mass is M , the metric function ϕ must satisfy the boundary condition, where

$$\exp(2\phi(R)) = 1 - \frac{2GM}{Rc^2},$$

which ensures continuity with Schwarzschild’s solution for the space-time outside a spherically symmetric object.

The above boundary condition implies that at the surface of the star, the gravitational potential $\phi(R)$ is related to the total mass M of the star and its radius R . The above condition aligns with the Schwarzschild’s metric, describing the gravitational field outside the star.

Using the above metric, the interior solution of Einstein’s field equations [7] in General Relativity leads to the TOV equations, first-order differential equations describing the balance of forces within the star. These equations represent the hydrostatic equilibrium condition, where the outward pressure forces in each star layer balance the inward gravitational force.

The TOV equations under Einstein’s General Relativity [25] in standard form are as follows:

$$\frac{dm}{dr} = 4\pi r^2 \rho(r) \quad (2)$$

$$\frac{d\phi}{dr} = \frac{G(m(r) + 4\pi r^3 P/c^2)}{r(rc^2 - 2Gm(r))} \quad (3)$$

$$\frac{dP}{dr} = -c^2 \left(\rho(r) + \frac{P}{c^2} \right) \frac{d\phi}{dr}, \quad (4)$$

where, $m(r)$ is the total mass enclosed within radius r , $\rho(r)$ is the local mass density at radius r , and $4\pi r^2 \rho(r)$ represents the incremental mass in a spherical shell at radius r with thickness dr . $\phi(r)$ is the gravitational potential at radius r . The term $\frac{d\phi}{dr}$ represents the gradient of the gravitational potential and $P(r)$ is the pressure at radius r .

The above equations are self-coupled and are solved employing a suitable EOS to determine the structure of a neutron star or other compact object. Usually, these differential equations are solved numerically starting at the object’s center, where initial conditions are defined ($P = P_c, r = 0$), and moving outward until the pressure, $P = 0$ [27] i.e., it falls to zero indicating the star’s outer boundary. Here, P_c represents the central pressure. The object’s total mass is given by $m(R) = M$, where R

represents the star's entire radius.

This system of equations results:

1. The object's mass-radius relationship for different possible stars.
2. The potential, density, and pressure as function of a particular star's radial distance.

In contrast to Newtonian gravity, these equations provide a more accurate description of the internal structure and pressure balance of such objects by taking into account the effects of general relativity. These equations are solved using a specific EoS for the matter inside the object, which connects the pressure P and density ρ of the matter.

Since the TOV equations depict how the neutron stars balance massive relativistic gravitational forces with the forces arising due to internal pressures, these forces are essential for comprehending the structure and stability of these objects. They are also necessary for examining the effects of various EOSs on neutron star mass and radius, which sheds light on the characteristics of dense matter under extreme conditions. As we improve our understanding of materials at nuclear densities by comparing observational data on neutron star masses and radii against theoretical models, the mass-radius relationship derived from the TOV equations also constrains the potential EoS for neutron stars.

C. Modified TOV equations due to the magnetic field

The interior structure of magnetars is directly impacted by the strong magnetic fields that function as an extra source in the energy-momentum tensor. Due to this interaction, the magnetic field contributes to the star's internal energy density. Therefore, this input of magnetic energy must be considered in the TOV equations, which can contribute in balancing the inward gravitational force and outward pressure forces within the star. Hence, in the TOV equations for NSs with strong inside magnetic field, the matter density term must include a magnetic energy density term due to the impact of the presence of the magnetic field. Thus the modified TOV equations [24], including the magnetic field energy density term, are given as follows [16]:

$$\frac{dm}{dr} = 4\pi r^2 \left(\rho(r) + \frac{B^2}{8\pi c^2} \right) \quad (5)$$

$$\frac{d\phi}{dr} = \frac{G \left(m(r) + 4\pi r^3 \frac{P}{c^2} \right)}{r \left(rc^2 - 2Gm(r) \right)} \quad (6)$$

$$\frac{dP}{dr} = -c^2 \left(\rho(r) + \frac{B^2}{8\pi c^2} + \frac{P}{c^2} \right) \left(\frac{d\phi}{dr} - L(r) \right). \quad (7)$$

Here, most of the symbols used have already been described in the text except a few, which we describe below. $L(r)$ is the Lorentz force term [3], which represents the force exerted on charged particles by the magnetic field inside the star and is given by

$$L(r) = B_c^2 [-3.8x + 8.1x^3 - 1.6x^5 - 2.3x^7] \times 10^{-41}, \quad (8)$$

where $x = r/\bar{r}$ with \bar{r} as the mean radius (slightly larger than the star's actual radius) of the star arising due to the impact of the strong magnetic field inside the NSs. The symbol B_c is the central magnetic field.

D. Modified TOV equations due to the impact of modified gravity

The $f(R, T)$ gravity is an extension of the $f(R)$ gravity [8] that incorporates a dependence on the trace of the energy-momentum tensor T [28]. It is a General Relativity (GR) variation, first presented by T. Harko et al., in 2011. For $f(R, T)$ gravity, the action S is as follows:

$$S = \int \sqrt{-g} \left[\frac{1}{16\pi G} f(R, T) + \mathcal{L}_m \right] d^4x, \quad (9)$$

where $f(R, T)$ is an arbitrary function of the Ricci's scalar R and the trace T of the energy-momentum tensor, \mathcal{L}_m is the matter Lagrangian, and g is the determinant of the metric tensor $g_{\mu\nu}$.

The addition of T allows the theory to account for both curvature effects R and effects of matter, such as particle generation or quantum field interactions.

The modified Einstein field equations [29] in $f(R, T)$ gravity are obtained by modifying the action about the metric $g_{\mu\nu}$. These are as follows: [30]:

$$\begin{aligned} G_{\mu\nu} + (f_R - 1)R_{\mu\nu} - \frac{1}{2}g_{\mu\nu}f + (g_{\mu\nu}\square - \nabla_\mu\nabla_\nu) f_R \\ = 8\pi GT_{\mu\nu} + f_T T_{\mu\nu} + f_T \Theta_{\mu\nu} \end{aligned} \quad (10)$$

Here, $G_{\mu\nu}$ is the Einstein tensor

$$\begin{aligned} f_R &= \frac{\partial f}{\partial R}, \\ f_T &= \frac{\partial f}{\partial T}, \quad \square = g^{\mu\nu}\nabla_\mu\nabla_\nu, \text{ and} \\ \Theta_{\mu\nu} &= g^{\alpha\beta} \frac{\delta T_{\alpha\beta}}{\delta g^{\mu\nu}}. \end{aligned}$$

The metric for a spherically symmetric, non-rotating star is expressed as:

$$ds^2 = -e^{\nu(r)} dt^2 + e^{\lambda(r)} dr^2 + r^2 d\Omega^2 \quad (11)$$

The energy-momentum tensor is expressed as:

$$T_{\mu\nu} = (\rho + P)u_\mu u_\nu + P g_{\mu\nu}, \quad (12)$$

where ρ is the energy density, P is the pressure, and u^μ is the four-velocity of the fluid.

In this model, $f(R, T) = R + 2\lambda T$, [17] where λ is a modified gravity parameter, R is the Ricci scalar, and T is the trace of the energy-momentum tensor.

The modified TOV equations in GUs (i.e., $G = c = 1$) are written as follows:

$$\frac{dm}{dr} = 4\pi r^2 \left(\rho + \frac{B^2}{8\pi} \right) - \frac{2\lambda T r^2}{4}. \quad (13)$$

$$\frac{d\phi}{dr} = \frac{\left[m + 4\pi r^3 P + \frac{r^3}{2} \left(\frac{2\lambda T}{2} + \left(\rho + \frac{B^2}{8\pi} + P \right) 2\lambda \right) \right]}{r^2 \left(1 - \frac{2m}{r} \right)}, \quad (14)$$

$$\frac{dP}{dr} = - \left(\rho + \frac{B^2}{8\pi} + P \right) \left(\frac{d\phi}{dr} - \mathbf{L} \right), \quad (15)$$

where, $T = - \left(\rho + \frac{B^2}{8\pi} \right) + 3P$.

By solving the above equations, we calculated the mass and profile of neutron stars using boundary conditions. At $r = 0$: $m(0) = 0$, $\rho(0) = \rho_c$ (central density) and at the stellar surface ($r = R$): $P(R) = 0$.

E. Cooling of Neutron Stars

The primary mechanism responsible for NSs cooling at early times and high temperature stage is due to the neutrino [31, 32] and photon emission. The NSCool code [33–35] is a computational tool to model the thermal evolution of neutron stars and can be used to perform cooling simulations of the stars. It includes the energy balance and heat transport equations [36] by considering a few cooling mechanisms [37], such as neutrino emission [38], photon radiation, and heat conduction. The Newtonian formulation gives the following equation:

$$C_v \frac{dT_b^\infty}{dt} = -L_\nu^\infty(T_b^\infty) - L_\gamma^\infty(T_s) + H, \quad (16)$$

where C_v represents the total specific heat, L_ν^∞ represents the neutrino luminosity, L_γ^∞ represents the surface photon luminosity, and H indicates all potential [39] contributions arising due to heating processes outside NS. T_s is the temperature at the surface, while T_b^∞ is the temperature inside at any location. This yields the photon luminosity: $L_\gamma^\infty = 4\pi\sigma R^2(T_s^\infty)^4$. σ shows the Stefan-Boltzmann constant, and the star's radius is shown by R . The relationship between the redshifted temperature and the surface temperature measured at infinity is as follows: $T_s^\infty = T_s \sqrt{1 - \frac{2GM}{c^2 R}}$. Since the external observer is at infinity and measures these quantities on the redshifted scale, the superscript infinity (∞) is used here.

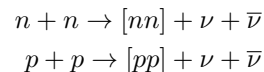
$T_s^\infty/T_s \sim 0.7$ is the usually used relation. Here, we assume $H = 0$. It has been assumed that core matter inside the NS lies in the superfluid state, provided the inside NS temperature is equal to or smaller than the superfluid critical temperature.

F. Neutrino emission inside NS core

1. Cooper Pair Breaking and Formation process (PBF)

The pair-breaking and formation (PBF) process occurs inside the superfluid core of neutron stars [40]. Baryonic matter transitions to a superfluid state as the core temperature falls below the critical temperature T_c . This phase transition involves the formation of Cooper pairs among baryons, analogous to the pairing seen in superconducting materials. In the superfluid state, the thermal energy available within the star can occasionally break these Cooper pairs. This breaking and subsequent reformation of pairs releases energy in the form of neutrino emission [41].

The PBF process is considered a cooling mechanism of paramount importance because it represents a dominant cooling mechanism during certain phases of a neutron star's life, particularly after the star has cooled sufficiently and other forms of neutrino emission mechanisms have tampered off.



When the temperature falls below the critical temperature $T_c = 10^9$ K of neutron (and proton) superfluid, axial-vector currents drive the significant cooling of neutron stars (NSs) with superfluid inside the core by the neutron/proton-wave-coupled [42] of neutrinos in a neutron/proton 1S_0 -wave coupled superfluid is determined by:

$$\epsilon_\nu^s = \frac{5G_F^2}{14\pi^3} \nu_N(0) v_F(N)^2 T^7 I_\nu^s. \quad (17)$$

Here, the integral I_ν^s is:

$$I_\nu^s = z_N^7 \left(\int_1^\infty \frac{y^5}{\sqrt{y^2 - 1}} [f_F(z_N y)]^2 dy \right), \quad (18)$$

where ϵ_ν^s is the neutrino emissivity, G_F is Fermi's coupling constant ($G_F = 1.166 \times 10^{-5} \text{ GeV}^{-2}$), $z = \Delta(T)/T$ with $\Delta(T) = 3.06T_c \sqrt{1 - T/T_c}$. Here T_c is the critical neutron/proton superfluid temperature.

G. Neutrino emission inside NS crust

1. *e-e Bremsstrahlung process*

Neutrino emission rate

The electron-electron bremsstrahlung mechanism contributes significantly to cooling in a neutron star's crust, especially in the early phases of the star's life cycle. The electron gas becomes relativistic in the crust, a dense region with electron degeneracy where electrons occupy states up to the Fermi energy. Electron-electron scattering results due to the electromagnetic interaction acting between the electrons in this environment. The electrons trade virtual photons during these scattering events, and the extra energy is released as a neutrino-antineutrino pair. This weak interaction-driven process allows neutrinos to carry energy away from the star, leading to its cooling. Temperature, density, and other variables affect this process's effectiveness; bremsstrahlung works best at greater temperatures and electron degeneracy. In neutron stars, thermal relaxation between the crust and core is greatly accelerated by the electron-electron bremsstrahlung process, particularly in the inner crust where densities are highest. Neutron stars typically have high temperatures $T = 10^8$ K during the early cooling phase. Young neutron stars and accreting neutron stars, where accretion causes the crust to grow hot, nonetheless benefit from this cooling process [43].

The neutrino emission rate [44] for e-e Bremsstrahlung process is given by:

$$\epsilon_{\nu ee, \text{brem}} = 7.42 \times 10^{-2} G_F^2 Z^2 \alpha_e^4 n_I T^6 L. \quad (19)$$

Here, $\alpha_e = \frac{1}{137}$ is the QED fine structure constant, n_i is the nuclei number density, and L includes many-body adjustments to the process rate associated with nuclear correlations.

III. RESULTS AND DISCUSSIONS

Figure (1) shows the enclosed mass of star as a function of radial distance from the center of a neutron star has been plotted for different values of the modified gravity parameter (λ) and with and without magnetic field scenarios, as shown in Figures 1(a), 1(b), and 1(c) for different EoSs, namely, APR, FPS, and SLY. Here we have considered a central magnetic field of $B = 10^{18}$ Gauss to determine the magnetic field profile at different locations inside NS from the center of star which is needed to solve the TOV equations. For both cases, i.e., with and without magnetic field scenarios, the mass-radial distance variation is plotted for three different values of the modified gravity parameter; $\lambda = 0, -\frac{1}{8\pi}, -\frac{2}{8\pi}, -\frac{3}{8\pi}$ to see the impact of modified gravity and magnetic field on the mass profile.

Magnetic Field and EoS Effects on Mass-Radial Distance Variation

On comparing the mass variation with radial distance with and without magnetic field case shown in Figure 1(a) for APR EoS, it is clear that due to the effect of the magnetic field, the mass-radial radius curves shift upward, suggesting that the magnetic field contributes significantly to sustaining a larger radius for a given mass. This effect is seen consistently across all values of λ . The magnetic field introduces additional pressure anisotropy, which counteracts the gravitational collapse and supports a more extended neutron star. Consequently, for a typical solar mass of 1.4, the radius increases when the magnetic field is present compared to the case without it. A similar magnetic field effect is observed for other FPS and SLY EoSs.

Modified Gravity and EOS Effects on mass profile

The influence of the modified gravity parameter λ can also be observed in both scenarios. The neutron star appears more compact for $\lambda = 0$, representing the standard general relativistic scenario. However, as λ decreases to negative values, the radius for a given mass consistently increases, indicating that weaker effective gravity results in a "fluffier" neutron star. This trend is evident in both the presence and absence of the magnetic field, with the effect being more pronounced in the $B = 0$ case where gravitational binding is reduced, and no additional magnetic pressure is available to stabilize the neutron star.

Magnetic Field and EoS Effects on Pressure-Radial Distance Variation

Figure (2) shows the influence of modified gravity and magnetic field can also be seen in the pressure versus radial distance plots as depicted in Figures 2(a), 2(b), and 2(c) for APR, FPS, and SLY EoSs, respectively.

It is clear from the pressure profile Figure 1(a) that the magnetic field significantly impacts the pressure at lower values radial distances from the center of the star, and this effect of the magnetic field decreases as we move toward the star's surface. It is also evident from the exact figure that magnetic field impact becomes more predominant for higher negative values of the modified gravity parameter λ . On comparing Figures 1(a), 1(b), and 1(c), although the qualitative variation of pressure versus radial distance does not change sizably when we move from APR to FPS or FPS to SLY EoSs, this impact slightly increases from APS to FPS EoSs and remains almost the same for SLY EOS.

Modified Gravity and EOS Effects on Pressure profile

As λ shifts towards more negative values from

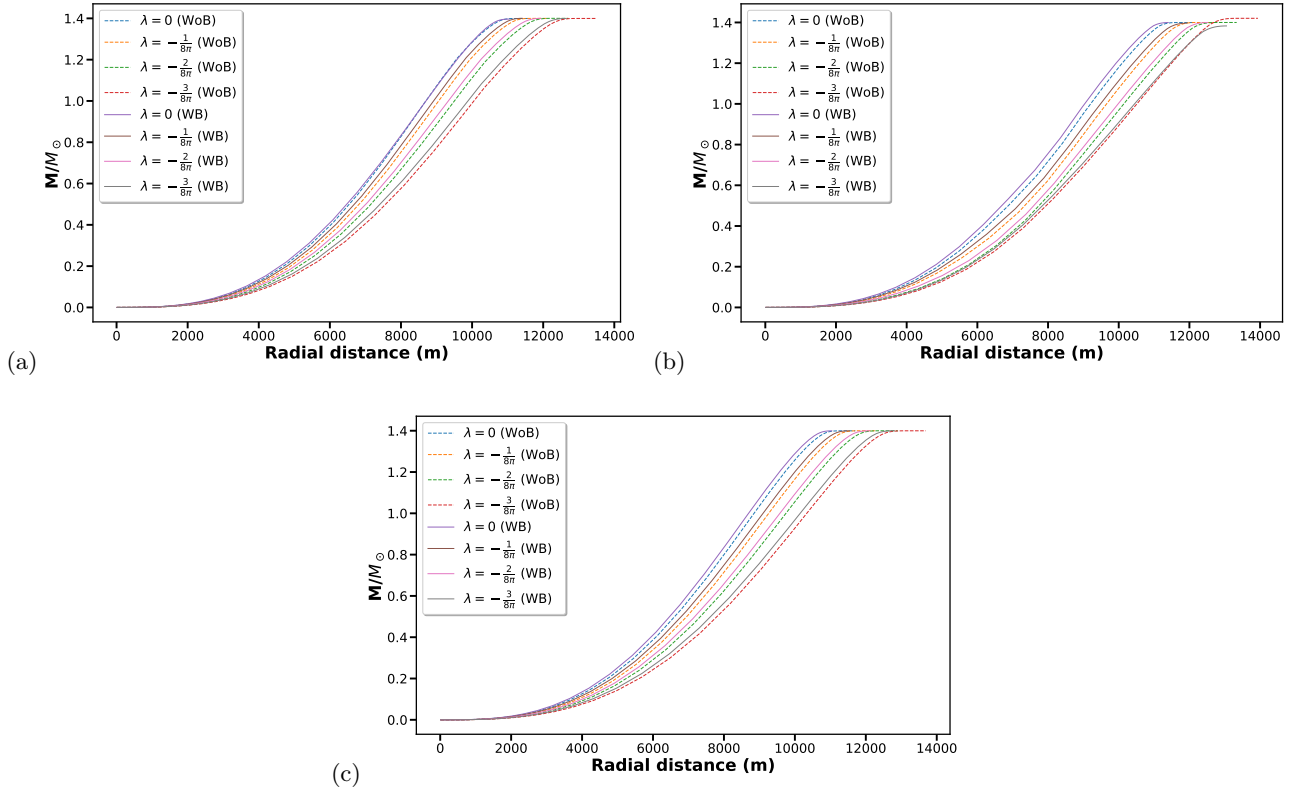
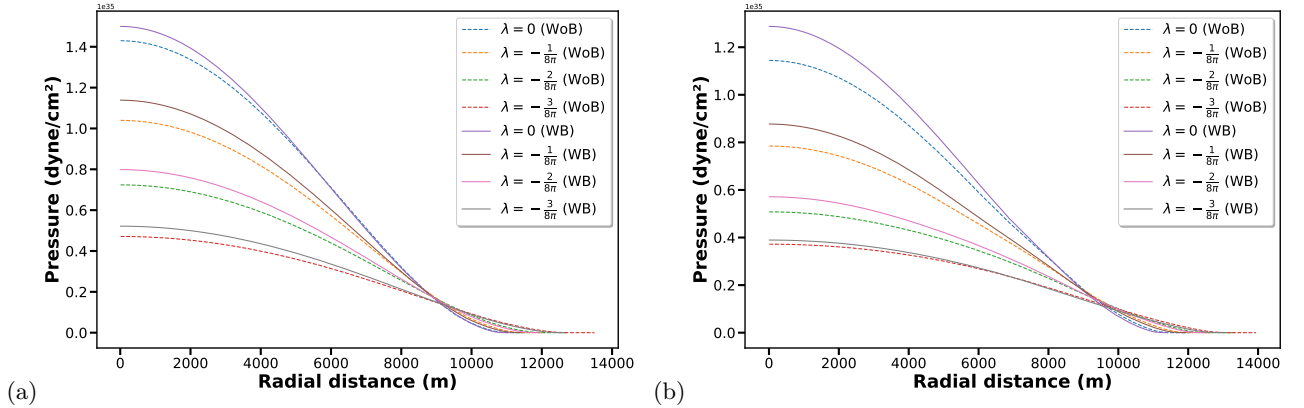


FIG. 1: The variation of mass with radial distance r for different equations of state (EoS): (a) APR, (b) FPS, and (c) SLY, both in the presence ($B = 10^{18}$ Gauss) and absence ($B = 0$) of magnetic fields for neutron stars of $1.4 M_{\odot}$. The cases without magnetic fields are labeled as “WoB” (Without Magnetic field) and the cases with magnetic fields are labeled as “WB” (With Magnetic field). The modified gravity parameter λ is set to $0, -\frac{1}{8\pi}, -\frac{2}{8\pi},$ and $-\frac{3}{8\pi}$.



$0, -\frac{1}{8\pi}, -\frac{2}{8\pi}, -\frac{3}{8\pi}$, the pressure gradient becomes steeper, implying that the reduction in gravitational pull leads to lower equilibrium pressures within the neutron star. This suggests that the stars for more negative λ values are less gravitationally bound, making it challenging to sustain high internal pressures, which aligns with the increased radial distance as observed in the mass-radial distance plots.

Surface temperature versus time plot for NS

In Figure (3), the predicted red-shifted surface temperature (T_s) of neutron stars (NSs) is plotted with and without a magnetic field for different values of the modified gravity parameter λ . These predictions are presented for three equations of state (EoS): APR, FPS, and SLY. Specifically, Figure 3(a) corresponds to the APR EoS, while Figures 3(b) and 3(c) depict results for FPS and SLY EoSs, respectively.

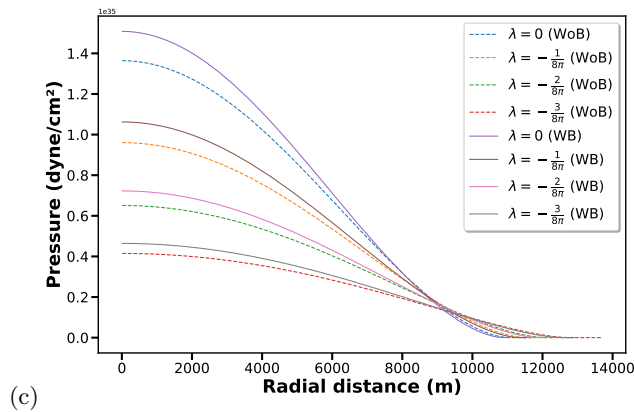


FIG. 2: The variation of pressure with radial distance r for different equations of state (EoS): (a) APR, (b) FPS, and (c) SLY, both in the presence ($B = 10^{18}$ Gauss) and absence ($B = 0$) of magnetic fields in neutron stars of $1.4 M_{\odot}$. The cases without magnetic fields are labeled as “WoB” (without magnetic field), and the cases with magnetic fields are labeled as “WB” (with magnetic field). The modified gravity parameter λ is set to, $-\frac{2}{8\pi}$, and $-\frac{3}{8\pi}$.

For the APR EoS, the least impact of the magnetic field and the modified gravity parameter λ on the surface temperature evolution is observed, as shown in Figure 3(a). In the presence of a magnetic field, T_s is initially predicted to be at higher temperatures during the early phase of the NS’s lifetime. The difference in surface temperature due to the magnetic field decreases as λ becomes more negative. This trend persists until approximately 100 years of the NS’s lifetime, beyond which the difference between the magnetic and non-magnetic cases remains minimal for all values of λ , including $\lambda = 0$.

In contrast, a significant difference in the T_s evolution between the magnetic and non-magnetic cases is evident for FPS and SLY EoSs. For FPS, as with APR, T_s initially remains at higher temperatures in the presence of a magnetic field. However, beyond 50 years, T_s decreases sharply with time, reflecting a sizable impact of the magnetic field across all values of λ . After 100 years, the magnetic field’s influence on T_s diminishes, and T_s evolves more slowly. Notably, the effect of the modified gravity parameter λ becomes more significant at later stages of the NS’s lifetime.

The SLY EoS presents a particularly non-trivial variation in T_s over time. For normal gravity conditions ($\lambda = 0$), the magnetic field’s influence is slightly more

pronounced during the initial NS evolution phases. Beyond 100 years, the impact of the magnetic fields shows a moderate effect on T_s values, which are lying below the non-magnetic case for the whole span of NS lifetime. For $\lambda = -1/8\pi$, the magnetic field impact is considerably larger after 100 years, with T_s values in the magnetic field case consistently lower than their non-magnetic counterparts. However, no sizable differences are observed for other λ values.

It is evident from **Table III** that the SLY EoS demonstrates a reasonable agreement between observed and predicted T_s values for non-zero λ values. This indicates that modified gravity, particularly in the presence of a magnetic field, works well for SLY EoS, yielding favorable results.

The parameter λ modifies the cooling rate by altering the internal thermodynamic properties of neutron stars. Figure (3) illustrates that larger absolute values of λ (both positive and negative) correspond to a slower cooling rate. This behavior suggests that stronger deviations from standard gravity (larger $|\lambda|$) lead to modifications in the equation of state, reduced neutrino emissivity, or altered energy transport processes, thereby flattening the T_s evolution curves and delaying the cooling process.

Luminosity versus time plot for NS

Figure (4) depicts photon and neutrino luminosities as a function of time for three EoSs, namely APR, FPS, and SLY, without a magnetic field. Photon luminosity for APR EoS with $\lambda = 0$ almost varies linearly till 1.5×10^2

years at a slower pace but beyond this time, it decreases still linearly but at a faster rate. An almost similar trend is observed for other values of λ at a slightly higher value, and it remains independent of non-zero λ values. Thus, modified gravity favors higher values of the photon luminosity. For the same EoS, neutrino

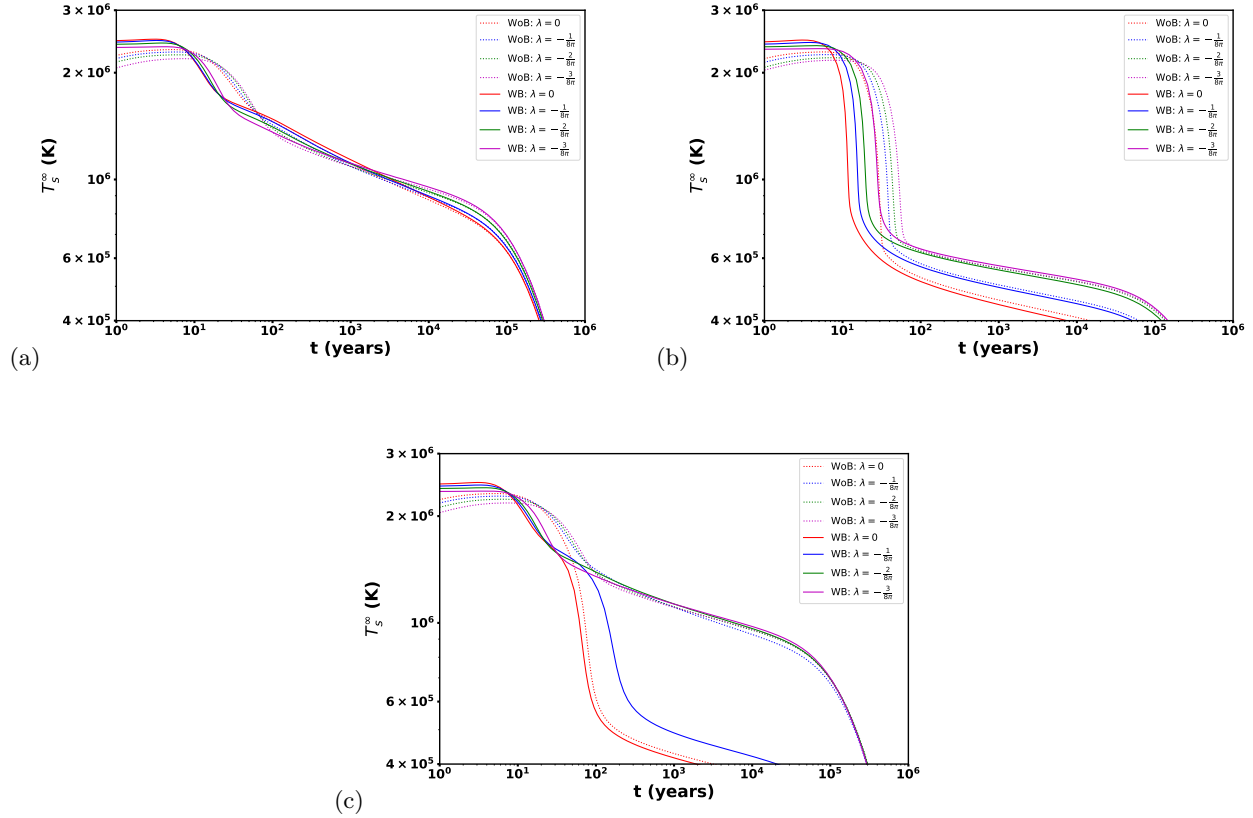
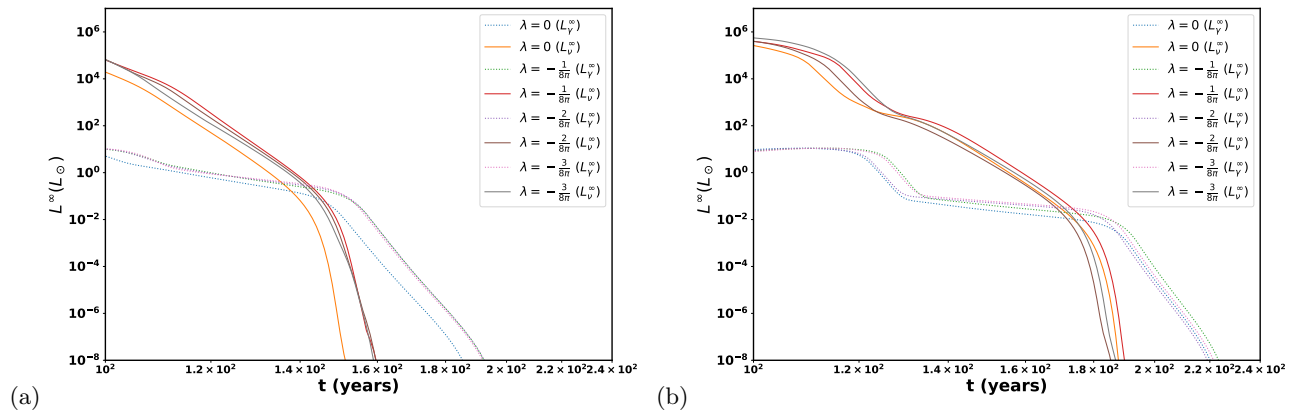


FIG. 3: The variation of effective surface temperature T_s^∞ with time t for different equations of state (EoS): (a) APR, (b) FPS, and (c) SLY, both in the presence ($B = 10^{18}$ Gauss) and absence ($B = 0$) of magnetic fields. The cases without magnetic fields are labeled as “WoB” (Without Magnetic field) and the cases with magnetic fields are labeled as “WB” (With Magnetic field). The modified gravity parameter λ is set to 0, $-\frac{1}{8\pi}$, $-\frac{2}{8\pi}$, and $-\frac{3}{8\pi}$.



luminosity is higher for several order of magnitude than photon luminosity at around 100 years of NSs lifetime.

For a normal Einstein gravity, neutrino luminosity decreases linearly faster than photon luminosity till 1.4×10^2 years. Beyond this time, it starts diminishing at a very faster rate. For non-zero values of λ , a similar trend is seen and remains independent with respect to λ values,

especially at later times.

Figure (5) depicts photon and neutrino luminosities as a function of time for three EoSs; namely APR, FPS and SLY EOSs with magnetic field, respectively. Figure 5(a) shows that photon luminosity varies linearly with time, very similar to the without magnetic field case, till around 1.6×10^2 years. This variation is not too sensitive with the modified gravity parameter during the

TABLE I: Comparison of observed surface temperature (T_s^∞) for three NSs with Age = 9.7×10^2 years[45, 46], 3.3×10^4 years,[47, 48] and 7.3×10^3 years,[49, 50] respectively, with the theoretically predicted values in the presence/absence of magnetic field for APR EoS

Age (years)	λ	T_s^∞ Without B (K)	T_e^∞ With B (K)	T_s^∞ Observed(K)
9.7×10^2	0	1.11×10^6	1.14×10^6	1.55×10^6
9.7×10^2	$-\frac{1}{8\pi}$	1.09×10^6	1.11×10^6	1.55×10^6
9.7×10^2	$-\frac{1}{2\pi}$	1.09×10^6	1.10×10^6	1.55×10^6
9.7×10^2	$-\frac{1}{3\pi}$	1.09×10^6	1.11×10^6	1.55×10^6
3.3×10^4	0	7.71×10^5	7.79×10^5	6.5×10^5
3.3×10^4	$-\frac{1}{8\pi}$	7.96×10^5	7.97×10^5	6.5×10^5
3.3×10^4	$-\frac{1}{2\pi}$	8.28×10^5	8.30×10^5	6.5×10^5
3.3×10^4	$-\frac{1}{3\pi}$	8.51×10^5	8.60×10^5	6.5×10^5
7.3×10^3	0	9.03×10^5	9.22×10^5	1.0×10^6
7.3×10^3	$-\frac{1}{8\pi}$	9.15×10^5	9.23×10^5	1.0×10^6
7.3×10^3	$-\frac{1}{2\pi}$	9.38×10^5	9.48×10^5	1.0×10^6
7.3×10^3	$-\frac{1}{3\pi}$	9.58×10^5	9.73×10^5	1.0×10^6

TABLE II: Comparison of observed surface temperature (T_s^∞) for three NSs with Age = 9.7×10^2 years,[45, 46] 3.3×10^4 years,[47, 48] and 7.3×10^3 years,[49, 50] respectively, with the theoretically predicted values in the presence/absence of magnetic field for FPS EoS

Age (years)	λ	T_s^∞ Without B (K)	T_e^∞ With B (K)	T_s^∞ Observed(K)
9.7×10^2	0	4.58×10^5	4.44×10^5	1.55×10^6
9.7×10^2	$-\frac{1}{8\pi}$	5.05×10^5	4.97×10^5	1.55×10^6
9.7×10^2	$-\frac{1}{2\pi}$	5.62×10^5	5.56×10^5	1.55×10^6
9.7×10^2	$-\frac{1}{3\pi}$	5.64×10^5	5.72×10^5	1.55×10^6
3.3×10^4	0	3.79×10^5	3.65×10^5	6.5×10^5
3.3×10^4	$-\frac{1}{8\pi}$	4.24×10^5	4.16×10^5	6.5×10^5
3.3×10^4	$-\frac{1}{2\pi}$	4.83×10^5	4.73×10^5	6.5×10^5
3.3×10^4	$-\frac{1}{3\pi}$	4.86×10^5	4.92×10^5	6.5×10^5
7.3×10^3	0	4.15×10^5	4.01×10^5	1.0×10^6
7.3×10^3	$-\frac{1}{8\pi}$	4.62×10^5	4.53×10^5	1.0×10^6
7.3×10^3	$-\frac{1}{2\pi}$	5.23×10^5	5.13×10^5	1.0×10^6
7.3×10^3	$-\frac{1}{3\pi}$	5.24×10^5	5.30×10^5	1.0×10^6

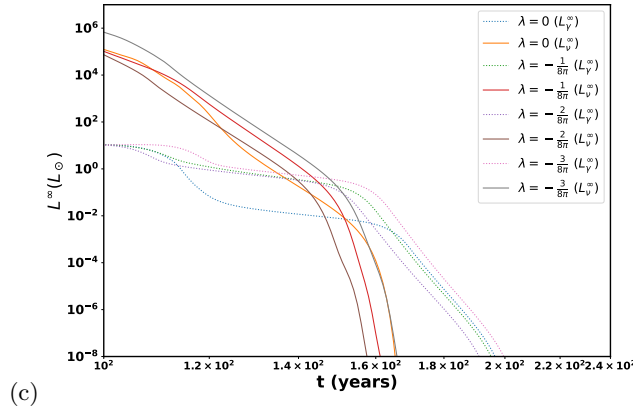


FIG. 4: Luminosity variation with time for APR, FPS, and SLY EoS without magnetic fields

initial phases of the NSs lifetime but beyond 1.6×10^2 years, it becomes quite sensitive to the λ parameter. On comparing Figures (4) & (5), it is clear that the

magnetic field effect on photon luminosity increases with an increase in λ parameter towards more negative values. Moreover, under the effect of the magnetic field,

TABLE III: Comparison of observed surface temperature (T_s^∞) for three NSs with Age = 9.7×10^2 years,[45, 46] 3.3×10^4 years,[47, 48] and 7.3×10^3 years,[49, 50] respectively, with the theoretically predicted values in the presence/absence of magnetic field for SLY EoS

Age (years)	λ	T_s^∞ Without B (K)	T_e^∞ With B (K)	T_s^∞ Observed(K)
9.7×10^2	0	4.30×10^5	4.17×10^5	1.55×10^6
9.7×10^2	$-\frac{1}{8\pi}$	1.10×10^6	4.91×10^5	1.55×10^6
9.7×10^2	$-\frac{1}{8\pi^2}$	1.11×10^6	1.13×10^6	1.55×10^6
9.7×10^2	$-\frac{1}{8\pi^3}$	1.11×10^6	1.13×10^6	1.55×10^6
3.3×10^4	0	3.44×10^5	3.34×10^5	6.5×10^5
3.3×10^4	$-\frac{1}{8\pi}$	8.33×10^5	3.84×10^5	6.5×10^5
3.3×10^4	$-\frac{1}{8\pi^2}$	8.63×10^5	8.68×10^5	6.5×10^5
3.3×10^4	$-\frac{1}{8\pi^3}$	8.66×10^5	8.81×10^5	6.5×10^5
7.3×10^3	0	3.82×10^5	3.71×10^5	1.0×10^6
7.3×10^3	$-\frac{1}{8\pi}$	9.50×10^5	4.30×10^5	1.0×10^6
7.3×10^3	$-\frac{1}{8\pi^2}$	9.74×10^5	9.86×10^5	1.0×10^6
7.3×10^3	$-\frac{1}{8\pi^3}$	9.78×10^5	9.97×10^5	1.0×10^6

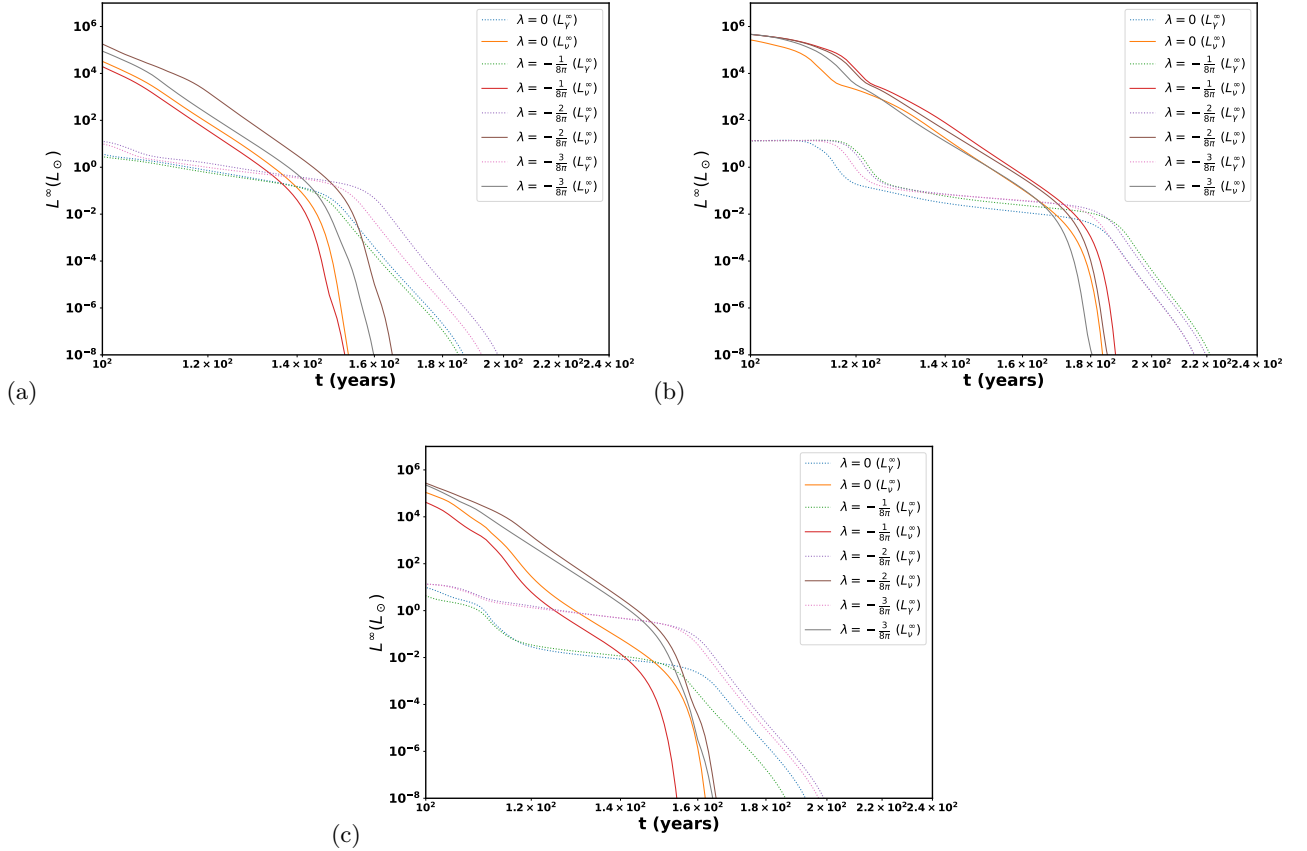


FIG. 5: Luminosity variation with time for APR, FPS, and SLY EoSs with magnetic fields

the sensitivity of the photon luminosity rises with the modified gravity parameter. For FPS EoS, luminosity remains flat initially, very similar to the no magnetic field counterpart, and after that, it drops sharply for a small interval of time. After that, it remains flat over a wide range of time and finally drops almost linearly. Neutrino luminosity decreases with time almost

monotonically over a long span of time till 1.8×10^2 years for with magnetic field. Beyond this time, it begins to decrease sharply.

Finally, Figure (5)(c) shows the luminosity of photon and neutrino variation with time with magnetic field for SLY EoS. From the figure, the magnetic field and

modified gravity effect are clearly seen in this case. However, the trend of variation with time remains the same with and without the magnetic field effect. For the non-zero modified gravity parameter λ , the magnetic field effect is significant for SLY EOS.

Similarly, under the effect of magnetic field for SLY EoS, photon luminosity changes with modified gravity parameter more significantly as compared to the case of non-magnetic field counterpart over a wide range of NSs lifetime. Furthermore, neutrino luminosity varies significantly with the change in the modified gravity parameter with a magnetic field compared to the case without a magnetic field. If we compare Figures (4)(c) & Figures (5)(c), for all values of λ , the impact of magnetic field is more significant as compared to other EoSs. Thus, for SLY EOS, the effect of magnetic field and modified gravity on photon/neutrino luminosity is clearly visible like APS EoS but unlike FPS EoS.

IV. CONCLUSION AND FUTURE OUTLOOK

In the current work, we have presented the emission and cooling properties of the NSs by employing the modified theory of gravity under the extreme conditions of matter density and magnetic field. The modified Tolman-Oppenheimer-Volkoff (TOV) system of equations has been employed in the current study. The extreme matter density and magnetic field inside the NSs provide a unique laboratory for studying fundamental physics. We here attempted to see how neutrinos and photon emissions from these compact objects are impacted by the modified TOV equations due to modified theory of gravity, $f(R, T)$ gravity or scalar-tensor theory. The strong

magnetic field effect with and without modified gravity parameter has also been studied here. Our analysis focuses on how these modifications impact NSs cooling rate, and emission processes, by determining neutrino and photon luminosities. We have also explored the implications of such modifications on the observational signatures such as observed NS's surface temperature by comparing our predicted values of surface temperature and observed values for three NS with and without including modified gravity and magnetic field effect. The present work contributes to the broader effort of linking predictions of the theoretical models with the observational data to refine our understanding of physics of the neutron stars and the fundamental forces governing the universe.

In future, our analysis can be extended for rotating and accreted neutron stars. A more thorough understanding of the interaction between rotation, accretion, and the equation of state (EoS) controlling the interior of neutron stars is anticipated under the modified gravity and strong magnetic field present inside the NSs. Investigation using the other EoSs, especially those that include hyperonic degree of freedom for the neutron star core matter will be carried out in our future communications.

Acknowledgments

One of the authors, Charul Rathod (CR), thanks DST New Delhi for providing financial support as DST-INSPIRE fellowship. CR also acknowledges the Birla Institute of Technology and Science - Pilani, Pilani Campus, Pilani - 333031 (Rajasthan) for the research facilities and the required administrative support.

-
- [1] V. M. Kaspi and A. M. Beloborodov, *Annual Review of Astronomy and Astrophysics* **55**, 261 (2017).
 - [2] J. M. Lattimer and M. Prakash, *Science* **304**, 536 (2004).
 - [3] V. Dexheimer, B. Franzon, R. Gomes, R. Farias, and S. Avancini, *Astronomische Nachrichten* **338**, 1052 (2017).
 - [4] J. Nättilä and J. J. Kajava (Springer, 2022), pp. 1–53.
 - [5] J. Piekarewicz (American Institute of Physics, 2009), vol. 1128, pp. 144–153.
 - [6] J. Kunz (Springer, 2023), pp. 293–313.
 - [7] A. Einstein, *Sitzungsber. Preuss. Akad. Wiss. Berlin (Math. Phys.)* **1915**, 844 (1915).
 - [8] T. P. Sotiriou and V. Faraoni, *Reviews of Modern Physics* **82**, 451 (2010).
 - [9] A. De Felice and S. Tsujikawa, *Living Reviews in Relativity* **13**, 1 (2010).
 - [10] A. M. Bauer, A. Cárdenas-Avendaño, C. F. Gammie, and N. Yunes, *The Astrophysical Journal* **925**, 119 (2022).
 - [11] N. Alex and T. Reinhart, *Physical Review D* **101**, 084025 (2020).
 - [12] F. W. Hehl, arXiv preprint gr-qc/9712096 (1997).
 - [13] G. Carvalho, R. Lobato, P. Moraes, J. D. Arbañil, E. Otoniel, R. Marinho, and M. Malheiro, *The European Physical Journal C* **77**, 1 (2017).
 - [14] M. G. Alford, L. Brodie, A. Haber, and I. Tews, *Physical Review C* **106**, 055804 (2022).
 - [15] D. Chatterjee, J. Novak, and M. Oertel, *Physical Review C* **99**, 055811 (2019).
 - [16] S. Yadav, M. Mishra, T. G. Sarkar, and C. R. Singh, *The European Physical Journal C* **84**, 225 (2024).
 - [17] P. Mahapatra and P. K. Das, arXiv preprint arXiv:2401.01321 (2024).
 - [18] A. Akmal, V. Pandharipande, and D. Ravenhall, *Physical Review C* **58**, 1804 (1998).
 - [19] M. Gusakov, A. Kaminker, D. G. Yakovlev, and O. Y. Gnedin, *Monthly Notices of the Royal Astronomical Society* **363**, 555 (2005).
 - [20] P. Haensel, J. Zdunik, and F. Douchin, *Astronomy & Astrophysics* **385**, 301 (2002).
 - [21] A. S. Schneider, C. Constantinou, B. Muccioli, and M. Prakash, *Physical Review C* **100**, 025803 (2019).
 - [22] E. Flowers, M. Ruderman, and P. Sutherland, *Astrophys-*

- ical Journal, vol. 205, Apr. 15, 1976, pt. 1, p. 541-544. **205**, 541 (1976).
- [23] A. Broderick, M. Prakash, and J. Lattimer, *The Astrophysical Journal* **537**, 351 (2000).
- [24] R. C. Tolman, *Physical Review* **55**, 364 (1939).
- [25] J. R. Oppenheimer and G. M. Volkoff, *Physical Review* **55**, 374 (1939).
- [26] K. Schleich and D. M. Witt, arXiv preprint arXiv:0910.5194 (2009).
- [27] J. B. Hartle and K. S. Thorne, *Astrophysical Journal*, vol. 153, p. 807 **153**, 807 (1968).
- [28] J. M. Pretel, S. E. Jorás, R. R. Reis, and J. D. Arbañil, *Journal of Cosmology and Astroparticle Physics* **2021**, 055 (2021).
- [29] T. Harko, F. S. Lobo, S. Nojiri, and S. D. Odintsov, *Physical Review D—Particles, Fields, Gravitation, and Cosmology* **84**, 024020 (2011).
- [30] Z. Haghani, T. Harko, and S. Shahidi, *Physics of the Dark Universe* **44**, 101448 (2024), 2301.12133.
- [31] R. Wijnands, N. Degenaar, and D. Page, *Journal of Astrophysics and Astronomy* **38**, 1 (2017).
- [32] A. Y. Potekhin, J. A. Pons, and D. Page, *Space Science Reviews* **191**, 239 (2015).
- [33] D. Page, U. Geppert, and F. Weber, *Nuclear Physics A* **777**, 497 (2006).
- [34] D. Page, *Astrophysics Source Code Library* pp. ascl-1609 (2016).
- [35] G. Brown, K. Kubodera, D. Page, and P. Pizzochero, *Physical Review D* **37**, 2042 (1988).
- [36] M. Buschmann, C. Dessert, J. W. Foster, A. J. Long, and B. R. Safdi, *Physical review letters* **128**, 091102 (2022).
- [37] M. Prakash, *Physics Reports* **242**, 297 (1994).
- [38] N. Iwamoto, L. Qin, M. Fukugita, and S. Tsuruta, *Physical Review D* **51**, 348 (1995).
- [39] M. V. Beznogov, J. Novak, D. Page, and A. R. Raduta, *The Astrophysical Journal* **942**, 72 (2023).
- [40] D. Page, J. M. Lattimer, M. Prakash, and A. W. Steiner, *The Astrophysical Journal* **707**, 1131 (2009).
- [41] D. Yakovlev, A. Kaminker, O. Y. Gnedin, and P. Haensel, *Physics Reports* **354**, 1 (2001).
- [42] L. Leinson, *Physics Letters B* **473**, 318 (2000).
- [43] D. Ofengeim, A. Kaminker, and D. Yakovlev, *European Physics Letters* **108**, 31002 (2014).
- [44] N. Iwamoto, *Physical review letters* **53**, 1198 (1984).
- [45] U. Geppert, M. Küker, and D. Page, *Astronomy & Astrophysics* **426**, 267 (2004).
- [46] J. A. O’Dea, F. Jenet, T.-H. Cheng, C. M. Buu, M. Beroiz, S. W. Asmar, and J. Armstrong, *The Astronomical Journal* **147**, 100 (2014).
- [47] F. Xu, J.-J. Geng, X. Wang, L. Li, and Y.-F. Huang, *Monthly Notices of the Royal Astronomical Society* **509**, 4916 (2022).
- [48] C.-Y. Ng, R. W. Romani, W. F. Brisken, S. Chatterjee, and M. Kramer, *The Astrophysical Journal* **654**, 487 (2007).
- [49] V. E. Zavlin, *The Astrophysical Journal* **665**, L143 (2007).
- [50] A. Danilenko, A. Kirichenko, R. Mennickent, G. Pavlov, Y. Shibanov, S. Zharikov, and D. Zyuzin, *Astronomy & Astrophysics* **540**, A28 (2012).